

DESIGN STUDIES OF THE REACCELERATOR RFQ AT NSCL*

Q. Zhao[†], V. Andreev, F. Marti, S.O. Schriber, X. Wu, R.C. York, National Superconducting Cyclotron Laboratory, Michigan State University, East Lansing, MI 48824, U.S.A.

Abstract

The reaccelerator system under development at the National Superconducting Cyclotron Laboratory (NSCL) will consist of a helium gas Radioactive Ion Beam (RIB) stopper, an electron beam ion trap, a cw radio frequency quadrupole (RFQ), and a superconducting linac to accelerate RIBs up to 3 MeV/u with charge-to-mass ratios (Q/A) of 0.2 - 0.4. The RFQ will operate in cw mode at a frequency of 80.5MHz to accelerate RIBs from 12 keV/u to 600 keV/u. An external multi-harmonic buncher will be used to achieve a small longitudinal emittance beam out of the RFQ. In this paper, we describe the design of the RFQ and the result of beam dynamics simulation.

INTRODUCTION

Radioactive Ion Beams (RIBs) are created at the National Superconducting Cyclotron Laboratory (NSCL) by the in-flight particle fragmentation method. A novel system that stops the RIBs in helium gas and reaccelerates them is proposed to provide opportunities for an experimental program ranging from low energy Coulomb excitation to transfer reaction studies of astrophysical reactions. The system will begin with a gas cell system to reduce the energy of the RIBs from 50 - 200 MeV/u to several keV/u. The stopped beam will be injected into and ionized to a high charge state ($0.2 < Q/A < 0.4$) in an electron beam ion trap (EBIT) charge breeder. After extraction from the EBIT with an energy of 12 keV/u, specific Q/A RIBs will be selected by a charge-state selection system and then be bunched and matched in a Low Energy Beam Transport (LEBT) system for injection into a cw Radio Frequency Quadrupole (RFQ). The 0.6 MeV/u output beam from the RFQ will be matched into two cryomodules of superconducting cavities for final acceleration up to 3 MeV/u. The beam will then be delivered to a target. A schematic layout of the reaccelerator is shown in Figure 1, and more information can be found in a separate paper [1].

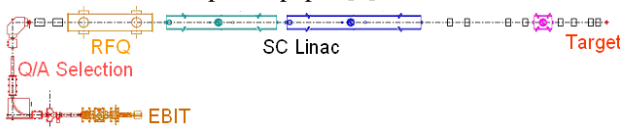


Figure 1: Schematic layout of the reaccelerator.

Elements of the experimental program require that the beam on target have simultaneously an energy spread of about 1 keV/u with a bunch length of approximately 1ns. This requirement demands a longitudinal beam emittance of $\sim 0.25 \pi$ -ns-keV/u. The space-charge effects will be negligible since the intensities of the RIBs will be low, and an external multi-harmonic buncher upstream of the RFQ will be used to produce a small longitudinal

emittance beam from RFQ [2]. Due to a larger intrinsic energy spread of the RIBs from EBIT ($\Delta E \sim \pm 25 \text{eV/u}$ for $Q/A=0.25$), the beam micro-bunch frequency should not be smaller than ~ 80 MHz, otherwise the longitudinal emittance of the bunched beam will be too large to achieve the required time and energy resolution on target. Therefore, a pre-buncher with three harmonics will operate at a fundamental frequency of 80.5 MHz.

An improved 4-vane RFQ structure with magnetic coupling windows [3,4] is proposed to provide a large mode separation and a compact structure with high shunt impedance. The RFQ will accelerate RIBs from 12 keV/u to 600 keV/u with operating frequency of 80.5 MHz. The input energy corresponding to $\sim 50 \text{kV}$ extraction voltage of EBIT is necessary to achieve reasonable transit time factors for the multi-harmonic buncher, while the output energy is required by the longitudinal beam dynamics of the downstream superconducting linac. The operating frequency is the same as the linac. For reliable cw operation, a moderate peak electric surface field of no more than 17 MV/m (or $\sim 1.6 \cdot E_{\text{kilpatrick}}$) was chosen for RIBs with the lowest $Q/A = 0.2$.

MULTIHARMONIC BUNCHER

To achieve a short bunch length with high bunching efficiency, a multiple-harmonic buncher is necessary. A least-square-fit method for phase within $\pm 130^\circ$ was used to obtain the optimized coefficients. The results of the harmonic coefficients for a two-, and three-harmonic buncher system are listed in Table 1.

Table 1: Voltage coefficients and bunching efficiencies for a two-, three-harmonic buncher.

Harmonics	U1	U2	U3	η (%)
2	1	0.303	0	77
3	1	0.351	0.115	82

A two harmonic buncher was found to provide a lower efficiency and larger longitudinal emittance compared to a three harmonic system, while the transit time factor is very low for the fourth harmonic and the efficiency of a four harmonic buncher was only a few percent higher, therefore a three harmonic buncher was chosen. The proposed buncher consists of two quarter-wave cavities. One cavity provides the fundamental (80.5 MHz) and the third harmonic. The other cavity provides the second harmonic. To achieve a uniform field distribution, all the harmonics are applied in one single gap with a pair of grids. Although the voltage coefficient is smaller for higher harmonics, the transit time factor is also lower. Therefore, the required rf power for each frequency is similar.

* Work supported by MSU and DOE

[†] zhao@nscl.msu.edu

RFQ CELL DESIGN

Since the beam is already bunched at the entrance of RFQ by an upstream multi-harmonic buncher, the RFQ cell design allowed a higher acceleration efficiency while maintaining the small longitudinal emittance of the core beam. In this design, an initial synchronous phase of -20° and a modulation factor of 1.15 were chosen. These values are a compromise to achieve a reasonable ratio between the longitudinal acceptance and emittance. Figure 2 shows the initial longitudinal distribution of a $Q/A=0.2$ beam at the RFQ entrance together with the RFQ longitudinal acceptance.

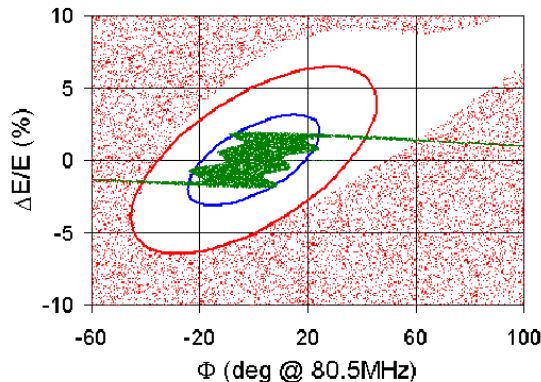


Figure 2: The Longitudinal acceptance (white area) of the RFQ and its maximum fitted ellipse (red line). Longitudinal distribution of a $Q/A=0.2$ beam (green dots) at the entrance of RFQ with a minimum ellipse (in blue line) fitted for the core particles are also shown.

The initial modulation factor was limited by the requirement of a maximum peak electric field in the entrance cells. The synchronous phase of -20° was kept constant throughout the RFQ, while the modulation factor was ramped quickly to ~ 2.6 in the first half meter and then kept constant. At the entrance of the RFQ, a 4-cell radial matching section was used followed by an entrance transition cell. The concept of the entrance transition cell is similar to that described in reference [5]. At the exit of the RFQ, a transition cell will bring the vanes to a quadrupole symmetry followed by an exit fringe-field region to obtain an output beam with similar Twiss parameters in both the horizontal and vertical planes to match the downstream solenoid focusing.

A constant inter-vane voltage of ~ 85 kV was adopted in the design for $Q/A = 0.2$ beam operation resulting in a vane length of 3.33 m. The focusing strength was held around 4.9 along the structure leading to a constant average aperture radius of 7.3 mm, and thereby keeping the capacitance almost independent of longitudinal position for easier cavity tuning. The transverse geometry of the vane-tip is circular with the same transverse radius of curvature throughout the RFQ making fabrication easier. The ratio between the vane tip transverse radius and the vane average radius was chosen to be 0.82 as a compromise between the peak electric field and the effect of multi-poles. The RFQ cell structure was generated by PARI [6] by an iterative cell-by-cell procedure. The

transverse phase advance per focusing period is approximately 30° , while the longitudinal one is around 20° . The transverse phase advance is larger than the longitudinal one to avoid a coupling resonance. Figure 3 shows the main parameters as a function of the RFQ length. The main design parameters of the RFQ are listed in Table 2.

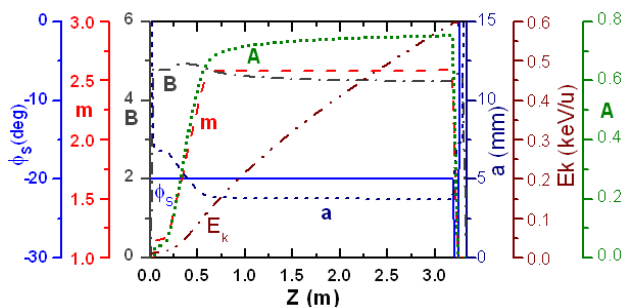


Figure 3: Evolution of the synchronous phase (ϕ_s), modulation factor (m), transverse focusing strength (B), minimum radius aperture (a), synchronous beam energy (E_k), and acceleration efficiency (A) along the RFQ.

Table 2: Main RFQ design parameters.

Name (unit)	Value
Frequency of operating mode (MHz)	80.5
Inter-vane voltage (kV)	86.2
Vane length (m)	3.33
Modulation factor	1.15 \rightarrow 2.58
Number of cells	94
Synchronous phase (degree)	-20
Mid-cell radial aperture (mm)	7.3
Vane tip transverse radius (mm)	6.0
Focusing strength	~ 4.9
Charge to mass ratio, Q/A	0.2
Input energy (keV/u)	12
Output energy (keV/u)	600
Effective transmission (%)	82
Peak electric field (MV/m)	16.7
Peak electric field ($E_{k\text{ilpatrick}}$)	1.6

RFQ BEAM DYNAMICS

The RIAPMTQ [7] code developed at LANL based on the standard PARMTEQ [6] code was used for the beam dynamics simulations through both the LEBT and RFQ. Figure 4 shows the particle distributions of a $Q/A=0.2$ beam at the entrance and exit of the RFQ with an intrinsic energy spread of $\pm 0.2\%$ from EBIT. Figure 5 shows the evolution of the transmission and rms emittances along the RFQ. About 82% of the beam was captured and accelerated by the RFQ. There is no transverse emittance growth in the RFQ. The longitudinal emittance of the core

particles (~90% of the total survived particles) at RFQ exit is preserved within 0.3π -keV/u-ns, while the full emittance to include the tail particles is about 2π -keV/u-ns. Since intrinsic energy spread from EBIT may be larger than $\pm 0.2\%$, this design can also accommodate such beams. Figure 6 shows the longitudinal phase space plots of a beam with an intrinsic energy spread of $\pm 0.5\%$ at the entrance and exit of the RFQ. The transmission efficiency is similar to that of $\pm 0.2\%$ case, but the output longitudinal emittance is larger because of the larger input. The beam dynamics through the RFQ are similar for other beams with different Q/A, provided the inter-vane voltage is scaled to account for the differences in the charge to mass ratio.

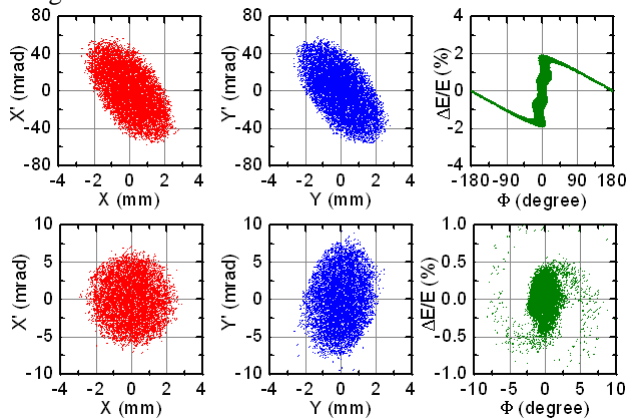


Figure 4: Phase space distributions of a Q/A=0.2 beam at the entrance (above) and the exit (below) of RFQ.

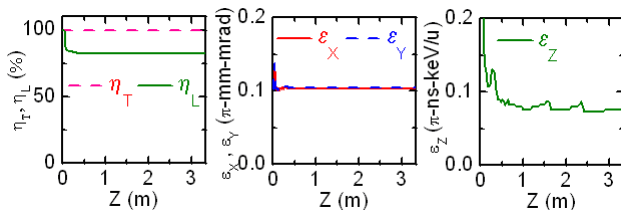


Figure 5: Evolution of the transmission (left) and rms normalized rms transverse emittance (middle), and longitudinal emittance along the RFQ.

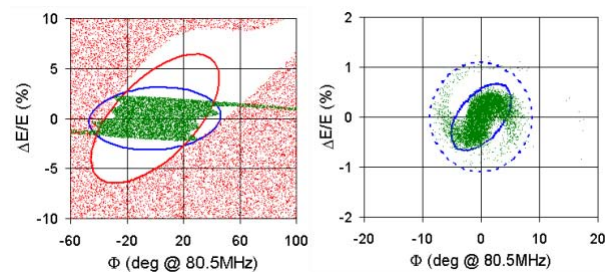


Figure 6: Longitudinal phase space plots of a 0.5% intrinsic energy spread beam at the entrance (left) and the exit (right) of RFQ.

RFQ RESONANT STRUCTURE

A resonant structure with high shunt impedance is preferred for cw RFQ operation. Although a 4-vane RFQ has lower power dissipation than that of a 4-rod RFQ, the

conventional 4-vane RFQs have parasitic modes close to the operating frequency and the structure becomes very large at low frequencies. Therefore, an improved 4-vane RFQ structure with magnetic coupling windows [3,4], which combines advantages of both the 4-vane and the 4-rod, is proposed. The windows on the vanes not only improve the azimuthal and longitudinal stability of the operating mode but also reduce the transverse dimensions of the RFQ resonator, while still maintaining a high shunt impedance. Figure 7 shows a simulated structure that is similar to another NSCL designed RFQ [8].

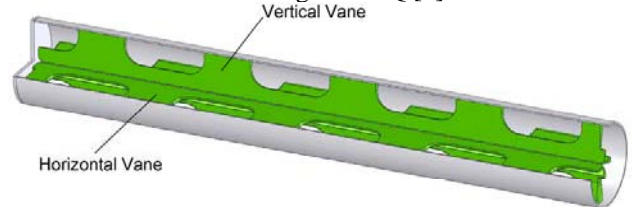


Figure 7: Schematic layout of the RFQ resonator.

SUMMARY

A cw RFQ for the reaccelerator has been designed. Beam dynamics simulations show the RFQ together with a three-harmonic buncher can produce the required output beam emittances. The 4-vane structure with window coupling has good mode separation, a compact size, and low power dissipation.

ACKNOWLEDGEMENTS

We are grateful to T.P. Wangler, K.R. Crandall, and J.H. Billen for their valuable discussions and providing the new versions of RFQ codes. We also thank A. Kolomiets, A. Schempp and D. Swenson for fruitful comments.

REFERENCES

- [1] X. Wu, et al., "Beam Dynamics Studies of the Accelerator System for the Reacceleration of Low Energy RIBs at the NSCL", these proceedings.
- [2] J.W. Staples, Part. Accel., 47(1994)191.
- [3] J.R. Delayen and W.L. Kennedy, "Design and Modeling of Superconducting RFQ Structures", LINAC'92, p.692, and K.W. Shepard, et al., "Design for a Superconducting Niobium RFQ Structure", LINAC'92, p.441.
- [4] V.A. Andreev and G. Parisi, "90°-apart-stem RFQ Structure for Wide Range of Frequencies", PAC'93, p.3124.
- [5] K.R. Crandall, "Ending RFQ Vanetips with Quadrupole Symmetry", LINAC'94, p.227
- [6] K.R. Crandall, et al., "RFQ Design Codes", LA-UR-96-183, LANL, Revised 2005.
- [7] R.W. Garnett, et al., "Advanced Beam-Dynamics Simulation Tools for RIA", PAC'05, p. 4218.
- [8] Q. Zhao, et al., "Design Improvement of the RIA 80.5 MHz RFQ", LINAC'04, p.599.